HHS Public Access

Author manuscript

Neuroscience. Author manuscript; available in PMC 2016 May 07.

Published in final edited form as:

Neuroscience. 2015 May 7; 293: 109–122. doi:10.1016/j.neuroscience.2015.02.042.

Coordinated Interaction of Down Syndrome Cell Adhesion Molecule (DSCAM) nd Deleted in Colorectal Cancer (DCC) with Dynamic TUBB3 Mediates Netrin-1-Induced Axon Branching

Huai Huang[†], **Qiangqiang Shao**[†], **Chao Qu**[†], **Tao Yang**, **Trisha Dwyer**, and **Guofa Liu**[‡]

Department of Biological Sciences, University of Toledo, 2801 West Bancroft St., Toledo, OH 43606, USA

Abstract

Modulation of actin and microtubule (MT) dynamics in neurons is implicated in guidance cue-dependent axon outgrowth, branching and pathfinding. Although the role of MTs in axon guidance has been well known, how extracellular guidance signals engage MT behavior in axon branching remains unclear. Previously, we have shown that TUBB3, the most dynamic β-tubulin isoform in neurons, directly binds to DCC to regulate MT dynamics in Netrin-1-mediated axon guidance. Here, we report that TUBB3 directly interacted with another Netrin-1 receptor DSCAM and Netrin-1 increased this interaction in primary neurons. MT dynamics were required for Netrin-1-promoted association of DSCAM with TUBB3. Knockdown of either DSCAM or DCC or addition of a function blocking anti-DCC antibody mutually blocked Netrin-1-induced interactions, suggesting that DSCAM interdependently coordinated with DCC in Netrin-1-induced binding to TUBB3. Both DSCAM and DCC were partially colocalized with TUBB3 in the axon branch and the axon branching point of primary neurons and Netrin-1 increased these colocalizations. Netrin-1 induced the interaction of endogenous DSCAM with polymerized TUBB3 in primary neurons and Src family kinases (SFKs) were required for regulating this binding. Knockdown of DSCAM only, DCC only or both was sufficient to block Netrin-1-induced axon branching of E15 mouse cortical neurons. Knocking down TUBB3 inhibited Netrin-1 induced axon branching as well. These results suggest that DSCAM collaborates with DCC to regulate MT dynamics via direct binding to dynamic TUBB3 in Netrin-1-induced axon branching.

Keywords

Axon Branching; Netrin-1; DSCAM; DCC; TUBB3; Microtubule Dynamics

[‡]To whom correspondence should be addressed: Guofa Liu, Department of Biological Sciences, University of Toledo, 2801 West Bancroft St., Toledo, OH 43606, USA, Tel: (419) 530-2869; Fax: (419) 530-7737; Guofa.Liu@utoledo.edu.

[†]H.H., S. Q. and C. Q. contributed equally to this work.

Conflict of interest

The authors declare no conflicts of interest.

1. Introduction

The formation of precise neuronal circuits in the developing nervous system relies on proper axon outgrowth, branching and pathfinding. Extensive branching and elaborate arborization from a single axon is essential for a neuron to connect with multiple synaptic targets (O'Leary et al., 1990, Yamahachi et al., 2009, Gibson and Ma, 2011, Kalil and Dent, 2014). Multiple extracellular molecules, such as axon guidance cues, growth factors and morphogens, are implicated in regulating axon branching during brain development (Gibson and Ma, 2011, Bilimoria and Bonni, 2013, Kalil and Dent, 2014). Netrin-1, a canonical axon guidance cue, can promote axon branching (Lai Wing Sun et al., 2011, Kalil and Dent, 2014). For example, local application of Netrin-1 promotes rapid branch formation along the axon shaft of dissociated hamster cortical neurons (Dent et al., 2004, Tang and Kalil, 2005), microinjection of Netrin-1 in the frog optic tectum induces dynamic axon branching *in vivo* (Manitt et al., 2009), and the expression of the N-terminal domain of the Netrin-1 homologue Uncoordinated-6 (UNC-6) induces axon branching of motoneurons in *C. elegans* (Lim et al., 1999). In the past two decades, a variety of signal transduction cascades underlying Netrin-1-mediated axon outgrowth and guidance have been identified, however, the mechanisms of the Netrin-1-induced axon branching are less known (Guan and Rao, 2003, Gibson and Ma, 2011, Kolodkin and Tessier-Lavigne, 2011, Lai Wing Sun et al., 2011, Kalil and Dent, 2014).

Assembling of appropriate receptor complexes is essential for Netrin-1 to differentially trigger intracellular signal transduction cascades in order to guide the growth cone steering (Quinn and Wadsworth, 2008, Lai Wing Sun et al., 2011, Liu and Dwyer, 2014). DSCAM collaborates with DCC to mediate Netrin-1-induced axon outgrowth and attraction (Ly et al., 2008, Liu et al., 2009), whereas Uncoordinated5 (UNC-5) associates either with DCC or DSCAM involved in axon repulsion (Keino-Masu et al., 1996, Kolodziej et al., 1996, Leonardo et al., 1997, Hong et al., 1999, Finger et al., 2002, Purohit et al., 2012). Loss of DCC function inhibits axon branching from dopaminergic (DA) neurons induced by Netrin-1 and causes defects in DA axon terminal arborization (Xu et al., 2010), suggesting that Netrin-1/DCC is required for DA axon branching during development. The isoform diversity of Drosophila DSCAM is involved in neuronal self-recognition, self-avoidance and axon collateral branching (Matthews et al., 2007, Schmucker, 2007, Soba et al., 2007, He et al., 2014). However, as a newly identified Netrin-1 receptor, whether DSCAM coordinates with DCC in Netrin-1-induced axon branching remains unclear.

Signal transduction cascades downstream of Netrin-1 eventually converge on modulating cytoskeleton dynamics including filamentous (F) actin and MTs to direct axon projection and branching (Lowery and Van Vactor, 2009, Stoeckli and Zou, 2009, Dent et al., 2011, Lai Wing Sun et al., 2011, Vitriol and Zheng, 2012, Kalil and Dent, 2014, Liu and Dwyer, 2014). MT dynamic instability and reorganization at axon branch points play an important role in the branch initiation and growth (Kalil and Dent, 2014). Recently, we found that DCC interacts directly with TUBB3, the most dynamic β-tubulin isoform in neurons, and Netrin-1 increases this interaction in primary cortical and commissural neurons (Qu et al., 2013a). Netrin-1 induces MT polymerization in developing neurons and promotes the interaction of DCC with dynamic TUBB3 (polymeric, not monomeric TUBB3) (Qu et al.,

2013a). Knockdown of TUBB3 blocks Netrin-1-induced axon outgrowth and pathfinding in the developing nervous system (Qu et al., 2013a). These results indicate that Netrin-1/DCC signaling can directly engage MT dynamics in axon guidance (Qu et al., 2013a). In this study, we sought to investigate whether DSCAM coordinates with DCC to couple Netrin-1 signaling to MT dynamics in Netrin-1-induced axon branching.

2. Experimental Procedures

2.1. Materials

Purified anti-DSCAM polyclonal antibody was described before (Liu et al., 2009, Purohit et al., 2012, Qu et al., 2013b). Other antibodies were obtained from commercial sources: rabbit anti-hemagglutinin (HA) (Santa Cruz, Lexington, NY), rabbit anti-Flag and rabbit anti-TUBB3 (Abcam, Cambridge, MA), mouse anti-DCC (BD Biosciences, Franklin Lakes, NJ), mouse anti-TUBB3 (Covance, Princeton, NJ), mouse anti-GST (Cell Signaling, Danvers, MA), mouse anti-Myc, and mouse functional blocking anti-DCC (EMD Millipore Bioscience, Billerica, MA), Alexa Fluor® 488 donkey anti-rabbit IgG (Jackson Immunoresearch, West Grove, PA), Alexa Fluor® 488 donkey anti-mouse IgG, Alexa Fluor® 647 donkey anti-rabbit IgG and Alexa Fluor® 633 goat anti-mouse IgG (Invitrogen, Carlsbad, CA), goat anti-rabbit IgG-HRP and bovine anti-mouse IgG-HRP (Santa Cruz, Lexington, NY). DAPI and BODIPY® 558/568 Phalloidin were obtained from Invitrogen. Taxol and Nocadozole were purchased from Cayman Chemicals (Ann Arbor, OH). PP2 and PP3 were obtained from Calbiochem (Rockland, MA).

Plasmids encoding short hairpin RNAs (the DCC shRNA, DSCAM shRNA, TUBB3 shRNA and the control shRNA) and human full-length TUBB3 and DSCAM have been described previously (Yu et al., 2002, Liu et al., 2009, Purohit et al., 2012, Qu et al., 2013a). The recombinant glutathione *S*-transferase fused DSCAM intracellular domain (DSCAM-ICD-GST) was produced from BL21 competent *E. coli* and pulled down through GST columns (Fisher, Pittsburg, PA). Eluted protein purity was analyzed by SDS-PAGE, followed by Coomassie blue staining. Purified TUBB3 was from Origene (Rockville, MD, USA). Netrin-1 protein and the sham-purified control were either obtained from R&D or purified with anti-Myc tag affinity matrix as described before (Liu et al., 2004, Liu et al., 2007, Li et al., 2008, Liu et al., 2009, Purohit et al., 2012, Qu et al., 2013a, Qu et al., 2013b).

2.2. Dissociated Primary Neuron Culture and Transfection

The procedures of primary neuron culture and nucleofection were performed as described previously with some modifications (Liu et al., 2004, Liu et al., 2007, Li et al., 2008, Liu et al., 2009, Purohit et al., 2012, Qu et al., 2013a, Qu et al., 2013b). Embryos were removed from anesthetized timed-pregnant mice of appropriate stages (E15 for cortical neurons and E13 for dorsal spinal cord neurons). The brain or the spinal cord were dissected in cold HBSS medium (Invitrogen) and meninges were removed. The explants were subsequently minced into small pieces with scissors and then trypsinized for 15 min at 37°C. After trituration, dissociated primary neurons were resuspended in DMEM supplemented with heat-inactivated fetal bovine serum (FBS, Invitrogen) and 20 U/ml of penicillin/streptomycin. Neurons were grown on poly-L-lysine (PLL, 62.5 μg/ml)-coated dishes

overnight at 37°C in a 5% CO2 incubator. For nucleofection, cortical neurons (4×10^6) were mixed with Venus YFP (1 μg) plus DCC shRNA (4 μg), DSCAM shRNA, TUBB3 shRNA or the control shRNAs, and immediately placed in Nucleofector (Amaxa Biosystems). The electroporation procedures were performed using O-005 program and transfected neurons immediately transferred from the cuvette into pre-warmed culture media. These dissociated neurons were then plated on PLL-coated (62.5 μg/ml) dishes and cultured in DMEM + 10% FBS + penicillin/streptomycin at 37 °C with 5% CO2. After 2 days of culture, primary neurons were lysed for immunoprecipitation and Western blot analysis.

2.3. Protein-Protein Interaction Analysis

HEK293 cells were transfected with polyethylenimine (PEI) and cultured 2 days after transfection as described previously (Qu et al., 2013a, Qu et al., 2013b). Dissociated primary neurons and HEK293 cells were starved for 6 h in serum-free DMEM media and followed by stimulated with purified Netrin-1 protein (50 ng/ml) or sham purified control. For immunoprecipitation, primary neurons from E15 mouse cortexes and HEK293 cells were lysed in mild lysis buffer (MLB: 20 mM Tris-Cl pH [7.4], 100 mM NaCl, 1% NP-40, 50 mM NaF, 1 mM sodium orthovanadate, 0.1 mM phenylmethylsulfonyl fluoride, and 1× protease inhibitor cocktail [Roche Molecular Biochemicals, Indianapolis, IN]) and dissociated neurons from E13 mouse dorsal spinal cords lysed with a modified RIPA buffer (50 mM Tris-HCl [pH 7.4], 150 mM NaCl, 0.5% deoxycholic acid, 0.5% Triton X-100, 1 mM PMSF, 1 mM sodium orthovanadate, 1×protease inhibitor cocktail [Roche Molecular Biochemicals]) as described previously (Liu et al., 2004, Liu et al., 2007, Li et al., 2008, Liu et al., 2009, Purohit et al., 2012, Qu et al., 2013a, Qu et al., 2013b). Cell lysates were immunoprecipitated with specific antibodies and protein A/G agarose beads (Santa Cruz Biotechnology) at 4°C for 2 h. For the immunoblotting, the washed immunoprecipitates and protein extracts from cell lysates were boiled in 1X SDS sample buffer for 5 min and separated with 7.5% SDS-polyacrylamide gel electrophoresis (SDS-PAGE). Western blots were visualized with the enhanced chemiluminescence (ECL) kit (Fisher) to detect specific proteins.

2.4. In Vitro Microtubule Cosedimentation Assay

Primary E15 mouse cortical neurons were cultured in the culture medium (DMEM + 10% FBS + penicillin/streptomycin) for 16 h and starved in the starvation medium (DMEM + 0.1%BSA + penicillin/streptomycin) for 6 h as previously described (Liu et al., 2004, Liu et al., 2007, Li et al., 2008, Liu et al., 2009, Purohit et al., 2012, Qu et al., 2013a, Qu et al., 2013b). PP2 (5 nM) or PP3 (5 nM) was added into the starvation medium for 6 h to examine effects of SFKs on MT dynamics. Primary neurons were incubated with Netrin-1 (500 ng/ml) or sham-purified control for 20 min and lysed in MLB buffer. Cell lysates were centrifuged at 100,000 × g for 1 h at 4 °C and the supernatant was incubated with 40 μM taxol or DMSO in PEMG buffer (100 mM PIPES, 1 mM EGTA, 1 mM MgSO4, 1 mM GTP, pH 6.8) at room temperature for 30 min. Polymerized microtubules were separated by centrifugation through a 10% sucrose cushion at 50,000 × *g* for 30 min at 4 °C and the pellet was resuspended with tubulin buffer (50 mM HEPES, 1 mM MgCl2, 1 mM EGTA, 10% glycerol, 150 mM KCl, 40 μM taxol, 1 mM GTP, 5 mM Mg-ATP, 1 mM PMSF, 1 ×

protease inhibitor mixture) as described previously. DSCAM and TUBB3 in the pellet and supernatant fractions were separated by SDS-PAGE and analyzed by Western blotting.

2.5. Colocalization Analysis

To determine the subcellular localization of DSCAM, DCC and TUBB3 proteins, dissociated neurons from E15 mouse cortexes or E11 mouse dorsal spinal cords were plated on PLL-coated (200 μg/ml) coverslips and cultured in the culture medium (DMEM + 10% FBS and penicillin/ streptomycin) at 37 °C with 5% CO_2 for 24 h. The culture medium was replaced by DMEM with B27 and penicillin/streptomycin with purified Netrin-1 (250 ng/ml). Primary neurons were cultured at 37 °C with 5% CO2 for 72 h and then fixed in pre-warmed 4% paraformaldehyde (PFA) in DMEM at 37 °C for 30 min. After permeabilized with PBST (0.5% Triton X-100 in PBS) for 15 min, neurons were blocked with the blocking buffer (0.25% BSA and 0.1% Triton in PBS) at room temperature for 30 min and incubated with primary antibody solution containing either mouse anti-DCC and rabbit anti-TUBB3 or rabbit anti-DSCAM and mouse anti-TUBB3 antibodies at 4°C overnight. Neurons were then incubated with fluorescent-labeled secondary antibody conjugates (Alexa Fluor® 488 donkey anti-rabbit IgG and Alexa Fluor® 633 goat anti-mouse IgG or Alexa Fluor® 488 donkey anti-mouse IgG and Alexa Fluor® 647 donkey anti-rabbit IgG) for 1 hour at 37 °C and mounted onto glass slides with Fluorogel (Electron Microscopy Sciences). Images were sequentially taken using a confocal microscope (Leica, TCS, SP8) and fluorescent signals acquired in a photon counting mode using Leica® HyD detector with same setting throughout each experiment. Axon branching points and branches longer than 10 μm long were selected as the regions of interest (ROIs). The Pearson Correlation Coefficient (PCC) of each ROI was calculated using the colocalization module of Leica confocal software. PCC values from different groups were analyzed using the Student's *t* test.

2.6. Analysis of cortical axon branching

Dissociated E15 mouse cortical neurons were plated on the PLL-coated (200 ng/ml) coverslips after nucleofection with Venus plus different shRNAs (control shRNAs, DCC shRNA, DSCAM shRNA, DCC shRNA and DSCAM shRNA, TUBB3 shRNA, and TUBB3 shRNA plus wild type human TUBB3) and cultured in DMEM with 10% FBS and penicillin/ streptomycin for 6 h. The culture medium was then replaced by DMEM with B27 and penicillin/ streptomycin and purified recombinant chicken Netrin-1 (250ng/ml) was applied 12 h after medium replacement. After 72 h of Netrin-1 stimulation, primary neurons were fixed in pre-warmed 4% PFA for 30 min, permeabilized and blocked in 0.3% Trition X-100 + 3% BSA in PBS, and incubated with primary mouse anti-Tau antibody overnight at 4°C. Cells were then incubated with Alexa Fluor® 633 goat anti-mouse IgG at 37°C for 1 h and stained with DAPI (1:1000 in PBS) for 10 min at room temperature. Neuron were then incubated with BODIPY® 558/568Phalloidin (1:100) at 37°C for 30 min and mounted with the Fluorgel on glass slides. Images were taken with a confocal microscope (Leica, TCS SP8). The axon branching point with a branch longer than 10 μm was measured using the NIH ImageJ program. Data were analyzed with one-way ANOVA and then followed up with Kruskal–Wallis test using GraphPad Prism Version 5.04 (GraphPad Software Inc.).

3. Results

3.1. DSCAM interacts with TUBB3

The direct binding of DCC and TUBB3 is required for Netrin attractive signaling and DSCAM collaborates with DCC involved in Netrin-1-induced axon outgrowth and guidance in the developing nervous system (Ly et al., 2008, Liu et al., 2009, Qu et al., 2013a, Qu et al., 2013b). To test whether endogenous DSCAM interacts with TUBB3, we carried out co-immunoprecipitation experiments with primary neurons from embryonic day 15 (E15) mouse cerebral cortexes. TUBB3 was readily detected in lysates that were immunoprecipitated with anti-DSCAM antibody, while TUBB3 was not present when primary antibody was omitted (Fig. 1A). To examine whether Netrin-1 regulates this interaction, we stimulated primary cortical neurons with Netrin-1 before carrying the co-immunoprecipitation experiments. Treatment with Netrin-1 increased the interaction of DSCAM with TUBB3 (Fig. 1A, quantification in Fig. 1C, upper panel). Netrin/DSCAM signaling is involved in spinal cord commissural axon outgrowth and pathfinding (Ly et al., 2008, Liu et al., 2009, Qu et al., 2013b). To determine whether endogenous DSCAM interacts with TUBB3 in developing spinal cord commissural neurons, primary neurons from the dorsal half of E13 mouse spinal cords were cultured and treated with Netrin-1. The cell extracts were immunoprecipitated with anti-DSCAM antibody before probing the blots with the anti-TUBB3 antibody. As expected, the immunoprecipitation results indicated endogenous DSCAM interacted with TUBB3 and Netrin-1 dramatically increased this interaction (Fig. 1B, quantification in Fig. 1C, lower panel). Time course experiments, both in E15 cortical (Fig. 1D) and E13 dorsal spinal cord neurons (Fig. 1E), indicated that Netrin-1 increased the interaction of TUBB3 with DSCAM within 5 min and the induction lasted up to 20 min after Netrin-1 stimulation (Fig. 1D–E). These results strongly suggest that DSCAM associates with TUBB3 in primary neurons.

To test whether DSCAM and TUBB3 could directly bind to each other, we carried out co-immunoprecipitation experiments in HEK293 cells that do not share the same signaling machinery with primary neurons. cDNAs expressing Flag–tagged DSCAM were co-transfected with HA-tagged human TUBB3 into HEK293 cells and anti-HA antibody was used to immunoprecipitate TUBB3, followed by probing the blots with anti-Flag antibody to detect DSCAM. Anti-HA antibody co-immunoprecipitated DSCAM-Flag, suggesting that TUBB3 may directly interact with DSCAM (Fig. 1F). To further determine this direct interaction, a purified fusion protein of the intracellular domain (ICD) of DSCAM and GST (DSCAM-ICD-GST) were incubated with purified human TUBB3. TUBB3 appeared to interact directly with the intracellular domain of DSCAM (Fig. 1G).

3.2. DSCAM coordinates with DCC in binding to TUBB3

Both DCC and DSCAM directly interact with TUBB3 and Netrin-1 increases these interactions (Fig. 1G) (Qu et al., 2013a). To determine whether these receptors may coordinate with each other in Netrin-1-induced binding to TUBB3, several short hairpin-based RNA interference constructs (shRNAs) were designed, targeting a sequence common to human and mouse DCC or DSCAM, and transfected into E15 mouse cortical neurons (Fig. 2A–D). One DCC shRNA, but not the control shRNA, significantly knocked down the

expression of endogenous DCC, but not DSCAM, in E15 cortical neurons (Fig. 2A). Knockdown of endogenous DCC or addition of a function blocking anti-DCC antibody was sufficient to block Netrin-1-induced interaction of DSCAM and TUBB3, whereas expression of the control shRNA did not affect the Netrin-1 effect (Fig. 2A–B), suggesting that DCC is required for the Netrin-1-induced interaction of DSCAM and TUBB3. Similarly, a DSCAM shRNA reduced the expression of DSCAM, but not DCC, in E15 cortical neurons, and knockdown of DSCAM inhibited Netrin-1-induced interaction of DCC with TUBB3 (Fig. 2C–D). These results indicate that DSCAM and DCC coordinate interdependently to associate with TUBB3 in Netrin-1 signaling.

3.3. Colocalization of TUBB3 with DSCAM and DCC in developing axon branches and growth cones

DCC colocalizes with TUBB3 in the growth cone of primary cortical and spinal cord commissural neurons (Qu et al., 2013a). To test whether TUBB3 is subcellularly colocalized with DSCAM in developing neurons, primary neurons from the E11 dorsal spinal cord and E15 cortex were cultured. Immunofluorescence localization showed that DSCAM partially overlapped with TUBB3 in the peripheral region of growth cones of E11 spinal cord commissural neurons and E15 cortical neurons (Fig. 3A–F). Partial overlap of TUBB3 with DSCAM was also observed at axon branching points as well as in axon branches of E15 mouse cortical neurons (Fig. 4A–C) and Netrin-1 stimulation increased these colocalizations (Fig. 4D–F, quantification of Pearson's correlation coefficient of DSCAM and TUBB3 in Fig. 4M). Similarly, DCC also partially overlapped with TUBB3 (Fig. 4G–I) and Netrin-1 enhanced this colocalization at axon branching points as well as in axon branches of E15 cortical neurons (Fig. 4J–L, quantification of Pearson's correlation coefficient of DCC and TUBB3 in Fig. 4N). These results suggest that TUBB3 may be involved in Netrin-1-induced axon branching during brain development.

3.4. Netrin-1-induced interaction of DSCAM with dynamic TUBB3

Modulation of MT dynamics in growth cones and developing branches plays an important role in axon guidance and branch formation (Dent et al., 2011, Kalil and Dent, 2014, Liu and Dwyer, 2014). To test whether MT dynamics is essential for the Netrin-1-induced interaction of DSCAM and TUBB3, primary E15 mouse cortical neurons were treated with a MT-stabilizing drug taxol and a MT-destabilizing drug nocodazole and the cell extracts were immunoprecipitated with anti-DSCAM antibody before probing the blots with the anti-TUBB3 antibody. As expected, Netrin-1 stimulation increased the binding of endogenous DSCAM and TUBB3 in primary neurons (Fig. 5A). Disruption of MT dynamics by both taxol and nocodazole blocked the Netrin-1-induced interaction (Fig. 5A), suggesting that modulation of MT dynamics is required for the Netrin-1 dependent binding of DSCAM and TUBB3. Tyrosine phosphorylation of endogenous TUBB3 induced by SFKs is crucial for Netrin/DCC signaling (Qu et al., 2013a). To determine whether Netrin-1-induced interaction of DSCAM and TUBB3 is dependent on SFKs, E15 mouse cortical neurons were incubated with PP2, an inhibitor of the SFKs, or PP3, an inactive control of PP2. Co-immunoprecipitation results showed that PP2, but not PP3, inhibited the Netrin-1-induced binding of DSCAM and TUBB3 (Fig. 5B), indicating that this interaction induced by Netrin-1 relies on SFKs.

MT dynamic instability is a continuous switching between polymerization and depolymerization at MT plus ends which results in monomeric and polymeric α- and β-tubulin isoforms. To further investigate whether DSCAM binds to monomeric or polymeric TUBB3 in Netrin signaling, we performed a MT cosedementation assay on E15 mouse cortical neuron cell lysates. In this assay, more polymerized TUBB3 subunits were in the pellet than those in the supernatant after treating the cell lysate with taxol to stabilize MTs, whereas more monomerized TUBB3 subunits were in the soluble supernatant than in the pellet without taxol because cell lysates on ice induces MT depolymerization (Fig. 5C). In the presence of taxol, DSCAM cosedimented with polymerized MT with a large quantity of DSCAM in the pellet (Fig. 5C–D). Netrin-1 stimulation further increased DSCAM and polymeric TUBB3 in the pellets (Fig. 5C and quantification in Fig. 5D–E). In contrast, in the absence of taxol, most of the endogenous DSCAM remained in the supernatants with or without Netrin-1 stimulation (Fig. 5C and quantification in Fig. 5D). These results suggest that Netrin-1 induces the interaction of endogenous DSCAM with polymerized TUBB3 in primary neurons via modulation of MT dynamics. To further determine whether SFKs are required for Netrin-1-induced interaction of endogenous DSCAM and dynamic TUBB3, dissociated E15 mouse cortical neurons were incubated with PP2 or PP3 with or without Netrin-1 treatment and the MT cosedimentation assay was performed. As expected, Netrin-1 increased the amount of DSCAM in the MT-sedimented pellets (Fig. 5F, quantification in Fig. 5G). PP2, but not PP3, inhibited the Netrin-1-induced cosedimentation of DSCAM with polymerized MTs in primary neurons (Fig. 5F, quantification in Fig. 5G). These results indicate that SFKs are essential for regulating the binding of DSCAM to dynamic TUBB3 in Netrin-1 signaling.

3.5. Both DSCAM and DCC are required for Netrin-1-induced axon branching

Netrin-1 can promote cortical axon branching (Dent et al., 2004, Tang and Kalil, 2005). To study whether DSCAM collaborates with DCC in Netrin-1-mediated axon branching, primary cortical neurons from E15 mouse embryos were transfected with a construct encoding Venus yellow fluorescent protein (Venus YFP) with either the control shRNA, DSCAM shRNA, DCC shRNA or DSCAM shRNA plus DCC shRNA together, as described previously (Liu et al., 2007, Li et al., 2008, Liu et al., 2009, Purohit et al., 2012, Qu et al., 2013a, Qu et al., 2013b). These neurons were incubated with purified Netrin-1 for 4 days. In neurons transfected with the control vector (Fig. 6A–B), axon branching was induced by Netrin-1: the total number of branching points of each axon was increased from 7.2 ± 0.7 without Netrin-1 to 18.8 ± 1.1 with Netrin-1 (Fig. 6G). Knockdown of DSCAM blocked Netrin-1-induced axon branching (Fig. 6C–D): in the absence of Netrin-1, the total number of branching points of each axon was 4.7 ± 0.4; with Netrin-1 treatment, the total number of branching points of each axon was 5.8 ± 0.6 (Fig. 6G). Comparing Netrin-1-induced axon branching from the control shRNA-transfected neurons to DSCAM shRNA-transfected neurons (Fig. 6G), the difference is statistically significant ($p < 0.0001$) (Fig.6B and 6G), suggesting that DSCAM is required for this process. A similar effect of DCC shRNA on Netrin-1-induced axon branching was observed after 4 days of RNAi transfection (Fig. 6E): the total number of branching points of each axon was 5.0 ± 0.5 without Netrin-1 and 6.8 ± 0.7 with Netrin-1, respectively (Fig. 6G). The axon branching promotion activity of Netrin-1 was inhibited by DCC shRNA compared to Netrin-1-induced axon branching from the

control shRNA-transfected neurons (Fig. 6G). Knockdown of both DSCAM and DCC also blocked Netrin-1-induced axon branching of primary cortical neurons (Fig. 6F): in the absence of Netrin-1, the total number of branching points of each axon was 3.8 ± 0.4; with Netrin-1 treatment, the total number of branching points of each axon was 4.4 ± 0.5. There is a statistical difference in Netrin-1-induced axon branching between the control shRNA-transfected neurons and DSCAM and DCC shRNAs-transfected neurons (Fig.6B and 6F–G). Together, these results indicate that DSCAM and DCC function interdependently in Netrin-1-induced axon branching of primary neurons.

3.6. TUBB3 is essential for Netrin-1-induced axon branching

To explore whether TUBB3 is involved in axon branching, Venus YFP was co-transfected with the control shRNA, TUBB3 shRNA or TUBB3 shRNA and wild type TUBB3 together into E15 cortical neurons. Primary neurons after transfection were cultured with or without Netrin-1 treatment for 4 days. As expected, Netrin-1 dramatically increased axon branching from neurons transfected with the control shRNA (Fig. 7A–B): the total number of branching points of each axon was increased from 6.0 ± 0.5 in the absence of Netrin-1 to 19.2 ± 1.2 in the presence of Netrin-1 (Fig. 7G). In neurons transfected with TUBB3 shRNA, Netrin-1-induced axon branching was abolished (Fig. 7C–D): the total number of branching points of each axon was 3.9 ± 0.4 without Netrin-1 and 4.5 ± 0.3 with Netrin-1, respectively (Fig. 7G). The difference of Netrin-1-induced axon branching between the control shRNA group and TUBB3 shRNA group (Fig. 7D) is statistically significant ($p < 0.0001$) (Fig. 7B, D and G). Importantly, the expression of wild type human TUBB3 rescued the effect of TUBB3 knockdown on Netirn-1-induced axon branching (Fig. 7E–G). In neurons transfected TUBB3 shRNA and wild type human TUBB3, the total number of branching points of each axon was increased from 6.6 ± 0.6 without Netrin-1 to 14.8 ± 0.9 with Netrin-1. These results indicate that TUBB3 is specifically involved in Netrin-1-induced cortical axon branching.

4. Discussion

In the nervous system, TUBB3 is the most dynamic β-tubulin isotype mainly expressed in neurons. We have recently shown that the direct interaction of DCC and dynamic TUBB3 couples Netrin-1 signaling to MT dynamics in axon outgrowth and pathfinding (Qu et al., 2013a). Here we report that DSCAM coordinates with DCC involved in Netrin-1-induced axon branching via directly binding to polymerized TUBB3. These results suggest that extracellular guidance cues may directly regulate MT dynamics via binding of guidance receptors to MT subunits, which is required for both axon guidance and branching.

4.1. Direct coupling of DSCAM/DCC signaling to MT dynamics via TUBB3 in Netrin-1-induced axon branching

The regulation of actin and MT dynamics in response to guidance cues plays an essential role in the formation, outgrowth and targeting of axon branches during brain development (Kalil et al., 2000, Kornack and Giger, 2005, Kalil and Dent, 2014). Although MT reorganization and dynamics in the axon shaft and growth cone are required for axon branching and terminal arborization (Yu and Baas, 1994, Dent et al., 1999, Gallo and

Letourneau, 1999, 2000, Dent and Kalil, 2001), whether signal transduction cascades downstream of guidance receptors directly couples MT dynamics in these processes is still unclear. Results from our recent work indicate that TUBB3 directly links DCC signaling to MT dynamics in Netrin-1-mediated axon outgrowth and pathfinding (Qu et al., 2013a). In this study, we have found that TUBB3 directly interacts with DSCAM *in vitro* and *in vivo* and Netrin-1 increases this interaction (Fig. 1). In growth cones of E15 cortical neurons and E11 spinal cord commissural neurons, TUBB3 partially colocalizes with DSCAM in the peripheral region of the growth cone including lamellipodia and filopodia (Fig. 3). Similarly, TUBB3 partially colocalizes with DSCAM and DCC in the axon branching points and branches of developing cortical neurons and Netrin-1 induces these colocalizations (Fig. 4). Disruption of MT dynamics either by taxol or nocodazole abolishes the Netrin-1-induced interaction of DSCAM and TUBB3, suggesting that MT dynamics is required for this induction (Fig. 5). DSCAM cosediments with stabilized MTs and polymerized TUBB3, and Netrin-1 increases the ratio of DSCAM and polymerized TUBB3 in the cell pellet versus the supernatant fraction compared to the control group without Netrin-1 (Fig. 5), suggesting that Netrin-1 regulates MT dynamics via binding of DSCAM with dynamic polymerized TUBB3 in MTs. Previous studies suggest that signaling pathways downstream of Netrin/DCC and Netrin/DSCAM are coordinated in the developing nervous system (Ly et al., 2008, Purohit et al., 2012, Qu et al., 2013b). Both DCC and DSCAM interact with TUBB3 and Netrin-1 increases these interactions in primary neurons. Interestingly, knockdown of DCC in dissociated cortical neurons or application of anti-DCC functional-blocking antibody to primary neuron culture results in loss of Netrin-1-induced interaction of DSCAM and TUBB3 (Fig. 2). Similarly, DSCAM knockdown also abolishes Netrin-1-induced DCC and TUBB3 interaction (Fig. 2). These results suggest that endogenous DCC and DSCAM mutually regulate MT dynamics in an interdependent manner in Netrin-1 signaling. In addition, our functional data indicate that TUBB3 is required for Netrin-1-induced axon branching (Fig. 7). These results indicate that Netrin-1 can directly regulate MT dynamics through coupling its receptors with TUBB3 to induce axon branching: DSCAM collaborates with DCC to serve as a platform recruiting polymerized TUBB3 and MTs in the axon branching point which may further stabilize newly-formed branches or filopodia against retraction and promote branch outgrowth in response to Netrin-1.

Both DSCAM and DCC belong to the immunoglobulin superfamily sharing similar protein structure. As a Netrin-1 receptor, DSCAM collaborates with DCC in Netrin-1-induced axon outgrowth and attraction (Ly et al., 2008, Liu et al., 2009, Qu et al., 2013b). In this study, we found that DSCAM collaborates with DCC interdependently to interact with dynamic TUBB3 involved in Netrin-1-induced axon branching. These results suggest that coordination of DSCAM with DCC is essential not only in Netrin-1-mediated axon attraction, but also in Netrin-1-induced axon branching. Interestingly, DSCAM knock-out mice do not exhibit aberrant commissural axon pathfinding (Palmesino et al., 2012), whereas results from RNAi studies in chick and mice as well as evidence in Drosophila clearly show that collaboration of DSCAM and DCC plays an essential role in Netrin-1 signaling (Andrews et al., 2008, Ly et al., 2008, Liu et al., 2009). The mechanisms underlying this disparity are still unknown. Netrin-1-mediated commissual axon outgrowth, branching and pathfinding in the developing nervous system requires the cooperation with

other signaling molecules, for instance, heparin sulphate proteoglycans, integrins, Shh, draxin, Slits and laminins (Charron et al., 2003, Dickson and Gilestro, 2006, Ahmed et al., 2011, Lai Wing Sun et al., 2011). It is possible that compensatory mechanisms of these related molecules or/and signal transduction components downstream of DCC and DSCAM after the loss of DSCAM may play an important role in this disparity. A recent study demonstrated that conditional deletion of DCC from forebrain neurons significantly reduced the amount of total Src protein, whereas NMDA receptor subunit GluN2B expression was increased in $DCC^{-/-}$ mice (Horn et al., 2013). Activities of Src and PLCγ1, two critical signal molecules downstream of Netrin signaling, were dramatically decreased in neurons lacking DCC (Horn et al., 2013). These results suggest that genetic removal of guidance receptors can regulate expression and activities of other related signal molecules, resulting in compensatory effects on certain phenotypes. Further studies are needed to determine whether $DSCAM^{-/-}$ mice share similar regulation mechanisms with $DCC^{-/-}$ mice in Netrin signaling.

4.2. Signaling pathways modulating MT dynamics in Netrin-1-induced axon branching

Netrin-1 can directly regulate MT dynamics through the coupling of its receptor DCC and DSCAM to TUBB3 during axon attraction and branching (Qu et al., 2013a, Liu and Dwyer, 2014). Previous studies have also shown that Netrin-1 induces DCC dimerization or/and the interactions of DCC with DSCAM and UNC5 to recruit several intracellular signaling molecules forming a complex, such as FAK, Fyn, Src and PAK1 (Stein et al., 2001, Li et al., 2004, Liu et al., 2004, Meriane et al., 2004, Ren et al., 2004, Lai Wing Sun et al., 2011, Purohit et al., 2012). Netrin-1 induces tyrosine phosphorylation of DSCAM, TUBB3 and Fyn (Liu et al., 2009, Qu et al., 2013a). Netrin-1-induced tyrosine phosphorylation of TUBB3 requires SFKs because inhibition of Src kinases by PP2 decreases Netrin-1-induced TUBB3 phosphorylation (Qu et al., 2013a). SFKs are required for Netrin-1-promoted interaction of DCC and DSCAM with TUBB3 in primary neurons (Fig. 5)(Qu et al., 2013a). Inhibition of SFK activities blocks Netrin-1-induced cosedimentation of DSCAM and DCC with polymerized TUBB3 and MTs (Fig. 5)(Qu et al., 2013a). These results suggest that SFKs are essential in regulating MT dynamics in Netrin-1 signaling, functioning as key signaling components of DCC/DSCAM/TUBB3 complex. SFKs play an important role in growth cone steering and axonal branching via regulating MT dynamics (Suter et al., 2004, Paveliev et al., 2007). Therefore, collaboration of DCC with DSCAM may serve as a signaling platform for recruitment of a multicomponent protein complex including polymerized TUBB3, SFKs and other key signaling molecules to directly modulate MT dynamics in Netrin-1-induced axon outgrowth, branching and turning.

MT dynamics is regulated by various microtubule associated proteins (MAPs) including severing, destabilizing, motor and MT plus-end tracking proteins. Several MAPs are involved in axon branching such as tau, MAP1B, end-binding protein 1 (EB1), EB3, adenomatous polyposis coli protein (APC), doublecortin (DCX), KIF2A and spastin or katanin (Kalil and Dent, 2014, Liu and Dwyer, 2014). MAP1B, a MT-stabilizing MAP highly expressed in the developing nervous system (Tucker et al., 1989), associates mainly with dynamic MTs and induces MT nucleation, polymerization and stabilization (Takemura et al., 1992, Vandecandelaere et al., 1996). As a regulator of MT stability and dynamics,

MAP1B plays an important role in axon outgrowth, branching and pathfinding during brain development (Lowery and Van Vactor, 2009, Dent et al., 2011, Kalil and Dent, 2014) and is involved in Netrin-1-mediated axonal outgrowth and guidance (Meixner et al., 2000, Tymanskyj et al., 2012). Netrin-1-directed axon outgrowth of developing neurons requires MAP1B phosphorylation through the activation of the serine/threonine kinases cyclin-dependent kinase 5 (CDK5) and glycogen synthase kinase3 (GSK3) (Del Rio et al., 2004). Dephosphorylated MAP1B increases MT stability, resulting in terminal remodeling of mossy fibres and axon branching (Goold et al., 1999, Kalil and Dent, 2014). Thus, it is likely that MAP1B plays an important role in both Netrin-1-mediated axon guidance and branching via modulation of MT dynamics.

Our recent studies have shown that c-Jun N-terminal kinase 1 (JNK1) is specifically involved in the coordination of DCC and DSCAM in Netrin-1-mediated axon outgrowth and attraction (Qu et al., 2013b). JNKs can regulate MAPs, such as DCX, stathmin and tau, to modulate MT dynamics and stability in the growth cone. A previous study demonstrated that JNK-stathmin pathway is involved in BDNF-mediated axon branching and DCX phosphorylation plays an important role in axon branching as well. It is plausible that the JNK-stathmin/DCX-MT pathway may be involved in Netrin-1-induced axon branching. Further studies are needed to clarify these possibilities.

4.3. Potential coordination of DSCAM and DCC signaling with MTs in dendritic arborization and synaptic formation

Proper dendritic growth, branching, arborization and synapse formation are essential for neurons to establish precise neuronal circuits in the developing nervous system. Previous studies have shown that alternative splice isoforms of Drosophila DSCAM are involved in dendritic branch formation (Hutchinson et al., 2014), self-avoidance and patterning (Schmucker et al., 2000, Zhu et al., 2006, Hattori et al., 2007, Hughes et al., 2007, Matthews et al., 2007, Soba et al., 2007, Wojtowicz et al., 2007) as well as synaptic targeting (Cvetkovska et al., 2013). Aplysia DSCAM mediates de novo and learning-related synapse formation (Li et al., 2009). Vertebrate DSCAM also contributes to lamina-specific synaptic connections in chick retina (Yamagata and Sanes, 2008), dendrite self-avoidance and mosaic tiling in the mouse retina (Fuerst et al., 2008, Fuerst et al., 2009) and dendrite arborization and spine formation in the developing mouse cortical pyramidal neurons (Maynard and Stein, 2012). Interestingly, DCC is enriched in dendritic spines of mouse pyramidal neurons and conditional deletion of DCC from neurons in the adult mouse forebrain impairs dendritic spine morphology with reduced spinal head size and neck width, long-term potential (LTP) and spatial and recognition memory (Horn et al., 2013). It has been known that MT dynamics in dendrites play an important role in dendritic spine formation and synaptic activity (Gu et al., 2008, Shirao and Gonzalez-Billault, 2013). However, the mechanisms of how these guidance receptors regulate MT dynamics to govern dendritic spine development remain unclear. Results from this study and our previous work indicate that DSCAM coordinates with DCC to regulate MT dynamics via directly binding to dynamic TUBB3 in Netrin signaling (Qu et al., 2013a). It is tempting to speculate that the binding of DCC and DSCAM to dynamic TUBB3 may directly couple their signaling to MT

dynamics to mediate dendritic branching, arborization and synapse formation and plasticity during brain development.

5. Conclusions

In the developing nervous system, modulation of microtubule dynamics plays an important role in axon outgrowth, branching and pathfinding. Our data have demonstrated that dynamic TUBB3 is a key component in coupling of DSCAM/DCC signaling to MT dynamics in Netrin-1-induced axon branching. These results suggest a functional model that dynamic MTs 'captured' by DSCAM or/and DCC via binding to polymerized TUBB3 at branching sites of axons lead to a differential increase in MT growth and stabilization at these sites in response to Netrin-1, which could promote axon branch formation and growth. Further studies are required to evaluate this model.

Acknowledgments

This work was partially supported by the National Institute of Health (G.L.) and the Whitehall Foundation (G.L.).

Abbreviations

DCC	deleted in colorectal cancer
DSCAM	Down syndrome cell adhesion molecule
UNC5	uncoordinated-5
SFKs	Src family kinases
MAPs	microtubule associated proteins
EB	end-binding protein
DCX	doublecortin
APC	adenomatous polyposis coli protein
CDK5	cyclin-dependent kinase 5
GSK3	glycogen synthase kinase 3 and JNK1, c-Jun N-terminal kinase 1

References

Ahmed G, Shinmyo Y, Ohta K, Islam SM, Hossain M, Naser IB, Riyadh MA, Su Y, Zhang S, Tessier-Lavigne M, Tanaka H. Draxin inhibits axonal outgrowth through the netrin receptor DCC. J Neurosci. 2011; 31:14018–14023. [PubMed: 21957262]

Andrews GL, Tanglao S, Farmer WT, Morin S, Brotman S, Berberoglu MA, Price H, Fernandez GC, Mastick GS, Charron F, Kidd T. Dscam guides embryonic axons by Netrin-dependent and -independent functions. Development. 2008; 135:3839–3848. [PubMed: 18948420]

Bilimoria PM, Bonni A. Molecular control of axon branching. The Neuroscientist : a review journal bringing neurobiology, neurology and psychiatry. 2013; 19:16–24.

Charron F, Stein E, Jeong J, McMahon AP, Tessier-Lavigne M. The morphogen sonic hedgehog is an axonal chemoattractant that collaborates with netrin-1 in midline axon guidance. Cell. 2003; 113:11–23. [PubMed: 12679031]

Cvetkovska V, Hibbert AD, Emran F, Chen BE. Overexpression of Down syndrome cell adhesion molecule impairs precise synaptic targeting. Nat Neurosci. 2013; 16:677–682. [PubMed: 23666178]

Del Rio JA, Gonzalez-Billault C, Urena JM, Jimenez EM, Barallobre MJ, Pascual M, Pujadas L, Simo S, La Torre A, Wandosell F, Avila J, Soriano E. MAP1B is required for Netrin 1 signaling in neuronal migration and axonal guidance. Curr Biol. 2004; 14:840–850. [PubMed: 15186740]

Dent EW, Barnes AM, Tang F, Kalil K. Netrin-1 and semaphorin 3A promote or inhibit cortical axon branching, respectively, by reorganization of the cytoskeleton. J Neurosci. 2004; 24:3002–3012. [PubMed: 15044539]

Dent EW, Callaway JL, Szebenyi G, Baas PW, Kalil K. Reorganization and movement of microtubules in axonal growth cones and developing interstitial branches. J Neurosci. 1999; 19:8894–8908. [PubMed: 10516309]

Dent EW, Gupton SL, Gertler FB. The growth cone cytoskeleton in axon outgrowth and guidance. Cold Spring Harb Perspect Biol. 2011; 3

Dent EW, Kalil K. Axon branching requires interactions between dynamic microtubules and actin filaments. J Neurosci. 2001; 21:9757–9769. [PubMed: 11739584]

Dickson BJ, Gilestro GF. Regulation of commissural axon pathfinding by slit and its Robo receptors. Annu Rev Cell Dev Biol. 2006; 22:651–675. [PubMed: 17029581]

Finger JH, Bronson RT, Harris B, Johnson K, Przyborski SA, Ackerman SL. The netrin 1 receptors Unc5h3 and Dcc are necessary at multiple choice points for the guidance of corticospinal tract axons. J Neurosci. 2002; 22:10346–10356. [PubMed: 12451134]

Fuerst PG, Bruce F, Tian M, Wei W, Elstrott J, Feller MB, Erskine L, Singer JH, Burgess RW. DSCAM and DSCAML1 function in self-avoidance in multiple cell types in the developing mouse retina. Neuron. 2009; 64:484–497. [PubMed: 19945391]

Fuerst PG, Koizumi A, Masland RH, Burgess RW. Neurite arborization and mosaic spacing in the mouse retina require DSCAM. Nature. 2008; 451:470–474. [PubMed: 18216855]

Gallo G, Letourneau PC. Different contributions of microtubule dynamics and transport to the growth of axons and collateral sprouts. J Neurosci. 1999; 19:3860–3873. [PubMed: 10234018]

Gallo G, Letourneau PC. Neurotrophins and the dynamic regulation of the neuronal cytoskeleton. J Neurobiol. 2000; 44:159–173. [PubMed: 10934319]

Gibson DA, Ma L. Developmental regulation of axon branching in the vertebrate nervous system. Development. 2011; 138:183–195. [PubMed: 21177340]

Goold RG, Owen R, Gordon-Weeks PR. Glycogen synthase kinase 3beta phosphorylation of microtubule-associated protein 1B regulates the stability of microtubules in growth cones. J Cell Sci. 1999; 112(Pt 19):3373–3384. [PubMed: 10504342]

Gu J, Firestein BL, Zheng JQ. Microtubules in dendritic spine development. J Neurosci. 2008; 28:12120–12124. [PubMed: 19005076]

Guan KL, Rao Y. Signalling mechanisms mediating neuronal responses to guidance cues. Nat Rev Neurosci. 2003; 4:941–956. [PubMed: 14682358]

Hattori D, Demir E, Kim HW, Viragh E, Zipursky SL, Dickson BJ. Dscam diversity is essential for neuronal wiring and self-recognition. Nature. 2007; 449:223–227. [PubMed: 17851526]

He H, Kise Y, Izadifar A, Urwyler O, Ayaz D, Parthasarthy A, Yan B, Erfurth ML, Dascenco D, Schmucker D. Cell-intrinsic requirement of Dscam1 isoform diversity for axon collateral formation. Science. 2014; 344:1182–1186. [PubMed: 24831526]

Hong K, Hinck L, Nishiyama M, Poo MM, Tessier-Lavigne M, Stein E. A ligand-gated association between cytoplasmic domains of UNC5 and DCC family receptors converts netrin-induced growth cone attraction to repulsion. Cell. 1999; 97:927–941. [PubMed: 10399920]

Horn KE, Glasgow SD, Gobert D, Bull SJ, Luk T, Girgis J, Tremblay ME, McEachern D, Bouchard JF, Haber M, Hamel E, Krimpenfort P, Murai KK, Berns A, Doucet G, Chapman CA, Ruthazer ES, Kennedy TE. DCC expression by neurons regulates synaptic plasticity in the adult brain. Cell reports. 2013; 3:173–185. [PubMed: 23291093]

Hughes ME, Bortnick R, Tsubouchi A, Baumer P, Kondo M, Uemura T, Schmucker D. Homophilic Dscam interactions control complex dendrite morphogenesis. Neuron. 2007; 54:417–427. [PubMed: 17481395]

Hutchinson KM, Vonhoff F, Duch C. Dscam1 is required for normal dendrite growth and branching but not for dendritic spacing in Drosophila motoneurons. J Neurosci. 2014; 34:1924–1931. [PubMed: 24478371]

Kalil K, Dent EW. Branch management: mechanisms of axon branching in the developing vertebrate CNS. Nat Rev Neurosci. 2014; 15:7–18. [PubMed: 24356070]

Kalil K, Szebenyi G, Dent EW. Common mechanisms underlying growth cone guidance and axon branching. J Neurobiol. 2000; 44:145–158. [PubMed: 10934318]

Keino-Masu K, Masu M, Hinck L, Leonardo ED, Chan SS, Culotti JG, Tessier-Lavigne M. Deleted in Colorectal Cancer (DCC) encodes a netrin receptor. Cell. 1996; 87:175–185. [PubMed: 8861902]

Kolodkin AL, Tessier-Lavigne M. Mechanisms and molecules of neuronal wiring: a primer. Cold Spring Harb Perspect Biol. 2011; 3

Kolodziej PA, Timpe LC, Mitchell KJ, Fried SR, Goodman CS, Jan LY, Jan YN. frazzled encodes a Drosophila member of the DCC immunoglobulin subfamily and is required for CNS and motor axon guidance. Cell. 1996; 87:197–204. [PubMed: 8861904]

Kornack DR, Giger RJ. Probing microtubule +TIPs: regulation of axon branching. Curr Opin Neurobiol. 2005; 15:58–66. [PubMed: 15721745]

Lai Wing Sun K, Correia JP, Kennedy TE. Netrins: versatile extracellular cues with diverse functions. Development. 2011; 138:2153–2169. [PubMed: 21558366]

Leonardo ED, Hinck L, Masu M, Keino-Masu K, Ackerman SL, Tessier-Lavigne M. Vertebrate homologues of C. elegans UNC-5 are candidate netrin receptors. Nature. 1997; 386:833–838. [PubMed: 9126742]

Li HL, Huang BS, Vishwasrao H, Sutedja N, Chen W, Jin I, Hawkins RD, Bailey CH, Kandel ER. Dscam mediates remodeling of glutamate receptors in Aplysia during de novo and learning-related synapse formation. Neuron. 2009; 61:527–540. [PubMed: 19249274]

Li W, Lee J, Vikis HG, Lee SH, Liu G, Aurandt J, Shen TL, Fearon ER, Guan JL, Han M, Rao Y, Hong K, Guan KL. Activation of FAK and Src are receptor-proximal events required for netrin signaling. Nat Neurosci. 2004; 7:1213–1221. [PubMed: 15494734]

Li X, Gao X, Liu G, Xiong W, Wu J, Rao Y. Netrin signal transduction and the guanine nucleotide exchange factor DOCK180 in attractive signaling. Nat Neurosci. 2008; 11:28–35. [PubMed: 18066058]

Lim YS, Mallapur S, Kao G, Ren XC, Wadsworth WG. Netrin UNC-6 and the regulation of branching and extension of motoneuron axons from the ventral nerve cord of Caenorhabditis elegans. J Neurosci. 1999; 19:7048–7056. [PubMed: 10436059]

Liu G, Beggs H, Jurgensen C, Park HT, Tang H, Gorski J, Jones KR, Reichardt LF, Wu J, Rao Y. Netrin requires focal adhesion kinase and Src family kinases for axon outgrowth and attraction. Nat Neurosci. 2004; 7:1222–1232. [PubMed: 15494732]

Liu G, Dwyer T. Microtubule dynamics in axon guidance. Neuroscience bulletin. 2014; 30:569–583. [PubMed: 24968808]

Liu G, Li W, Gao X, Li X, Jurgensen C, Park HT, Shin NY, Yu J, He ML, Hanks SK, Wu JY, Guan KL, Rao Y. p130CAS is required for netrin signaling and commissural axon guidance. J Neurosci. 2007; 27:957–968. [PubMed: 17251438]

Liu G, Li W, Wang L, Kar A, Guan KL, Rao Y, Wu JY. DSCAM functions as a netrin receptor in commissural axon pathfinding. Proc Natl Acad Sci U S A. 2009; 106:2951–2956. [PubMed: 19196994]

Lowery LA, Van Vactor D. The trip of the tip: understanding the growth cone machinery. Nat Rev Mol Cell Biol. 2009; 10:332–343. [PubMed: 19373241]

Ly A, Nikolaev A, Suresh G, Zheng Y, Tessier-Lavigne M, Stein E. DSCAM is a netrin receptor that collaborates with DCC in mediating turning responses to netrin-1. Cell. 2008; 133:1241–1254. [PubMed: 18585357]

Manitt C, Nikolakopoulou AM, Almario DR, Nguyen SA, Cohen-Cory S. Netrin participates in the development of retinotectal synaptic connectivity by modulating axon arborization and synapse formation in the developing brain. J Neurosci. 2009; 29:11065–11077. [PubMed: 19741113]

Matthews BJ, Kim ME, Flanagan JJ, Hattori D, Clemens JC, Zipursky SL, Grueber WB. Dendrite self-avoidance is controlled by Dscam. Cell. 2007; 129:593–604. [PubMed: 17482551]

Maynard KR, Stein E. DSCAM contributes to dendrite arborization and spine formation in the developing cerebral cortex. J Neurosci. 2012; 32:16637–16650. [PubMed: 23175819]

Meixner A, Haverkamp S, Wassle H, Fuhrer S, Thalhammer J, Kropf N, Bittner RE, Lassmann H, Wiche G, Propst F. MAP1B is required for axon guidance and Is involved in the development of the central and peripheral nervous system. J Cell Biol. 2000; 151:1169–1178. [PubMed: 11121433]

Meriane M, Tcherkezian J, Webber CA, Danek EI, Triki I, McFarlane S, Bloch-Gallego E, Lamarche-Vane N. Phosphorylation of DCC by Fyn mediates Netrin-1 signaling in growth cone guidance. J Cell Biol. 2004; 167:687–698. [PubMed: 15557120]

O'Leary DD, Bicknese AR, De Carlos JA, Heffner CD, Koester SE, Kutka LJ, Terashima T. Target selection by cortical axons: alternative mechanisms to establish axonal connections in the developing brain. Cold Spring Harb Symp Quant Biol. 1990; 55:453–468. [PubMed: 2132832]

Palmesino E, Haddick PCG, Tessier-Lavigne M, Kania A. Genetic analysis of DSCAM's role as a Netrin-1 receptor in vertebrates. The Journal of neuroscience : the official journal of the Society for Neuroscience. 2012; 32:411–416. [PubMed: 22238077]

Paveliev M, Lume M, Velthut A, Phillips M, Arumae U, Saarma M. Neurotrophic factors switch between two signaling pathways that trigger axonal growth. J Cell Sci. 2007; 120:2507–2516. [PubMed: 17646673]

Purohit AA, Li W, Qu C, Dwyer T, Shao Q, Guan KL, Liu G. Down syndrome cell adhesion molecule (DSCAM) associates with uncoordinated-5C (UNC5C) in netrin-1-mediated growth cone collapse. J Biol Chem. 2012; 287:27126–27138. [PubMed: 22685302]

Qu C, Dwyer T, Shao Q, Yang T, Huang H, Liu G. Direct binding of TUBB3 with DCC couples netrin-1 signaling to intracellular microtubule dynamics in axon outgrowth and guidance. J Cell Sci. 2013a; 126:3070–3081. [PubMed: 23641072]

Qu C, Li W, Shao Q, Dwyer T, Huang H, Yang T, Liu G. c-Jun N-terminal kinase 1 (JNK1) is required for coordination of netrin signaling in axon guidance. J Biol Chem. 2013b; 288:1883–1895. [PubMed: 23223444]

Quinn CC, Wadsworth WG. Axon guidance: asymmetric signaling orients polarized outgrowth. Trends Cell Biol. 2008; 18:597–603. [PubMed: 18951796]

Ren XR, Ming GL, Xie Y, Hong Y, Sun DM, Zhao ZQ, Feng Z, Wang Q, Shim S, Chen ZF, Song HJ, Mei L, Xiong WC. Focal adhesion kinase in netrin-1 signaling. Nat Neurosci. 2004; 7:1204–1212. [PubMed: 15494733]

Schmucker D. Molecular diversity of Dscam: recognition of molecular identity in neuronal wiring. Nat Rev Neurosci. 2007; 8:915–920. [PubMed: 18026165]

Schmucker D, Clemens JC, Shu H, Worby CA, Xiao J, Muda M, Dixon JE, Zipursky SL. Drosophila Dscam is an axon guidance receptor exhibiting extraordinary molecular diversity. Cell. 2000; 101:671–684. [PubMed: 10892653]

Shirao T, Gonzalez-Billault C. Actin filaments and microtubules in dendritic spines. J Neurochem. 2013; 126:155–164. [PubMed: 23692384]

Soba P, Zhu S, Emoto K, Younger S, Yang SJ, Yu HH, Lee T, Jan LY, Jan YN. Drosophila sensory neurons require Dscam for dendritic self-avoidance and proper dendritic field organization. Neuron. 2007; 54:403–416. [PubMed: 17481394]

Stein E, Zou Y, Poo M, Tessier-Lavigne M. Binding of DCC by netrin-1 to mediate axon guidance independent of adenosine A2B receptor activation. Science. 2001; 291:1976–1982. [PubMed: 11239160]

Stoeckli E, Zou Y. How are neurons wired to form functional and plastic circuits? Meeting on Axon Guidance, Synaptogenesis & Neural Plasticity. EMBO reports. 2009; 10:326–330. [PubMed: 19305387]

Suter DM, Schaefer AW, Forscher P. Microtubule dynamics are necessary for SRC family kinase-dependent growth cone steering. Curr Biol. 2004; 14:1194–1199. [PubMed: 15242617]

Takemura R, Okabe S, Umeyama T, Kanai Y, Cowan NJ, Hirokawa N. Increased microtubule stability and alpha tubulin acetylation in cells transfected with microtubule-associated proteins MAP1B, MAP2 or tau. J Cell Sci. 1992; 103(Pt 4):953–964. [PubMed: 1487506]

Tang F, Kalil K. Netrin-1 induces axon branching in developing cortical neurons by frequency-dependent calcium signaling pathways. J Neurosci. 2005; 25:6702–6715. [PubMed: 16014732]

Tucker RP, Garner CC, Matus A. In situ localization of microtubule-associated protein mRNA in the developing and adult rat brain. Neuron. 1989; 2:1245–1256. [PubMed: 2624748]

Tymanskyj SR, Scales TM, Gordon-Weeks PR. MAP1B enhances microtubule assembly rates and axon extension rates in developing neurons. Mol Cell Neurosci. 2012; 49:110–119. [PubMed: 22033417]

Vandecandelaere A, Pedrotti B, Utton MA, Calvert RA, Bayley PM. Differences in the regulation of microtubule dynamics by microtubule-associated proteins MAP1B and MAP2. Cell motility and the cytoskeleton. 1996; 35:134–146. [PubMed: 8894283]

Vitriol EA, Zheng JQ. Growth cone travel in space and time: the cellular ensemble of cytoskeleton, adhesion, and membrane. Neuron. 2012; 73:1068–1081. [PubMed: 22445336]

Wojtowicz WM, Wu W, Andre I, Qian B, Baker D, Zipursky SL. A vast repertoire of Dscam binding specificities arises from modular interactions of variable Ig domains. Cell. 2007; 130:1134–1145. [PubMed: 17889655]

Xu B, Goldman JS, Rymar VV, Forget C, Lo PS, Bull SJ, Vereker E, Barker PA, Trudeau LE, Sadikot AF, Kennedy TE. Critical roles for the netrin receptor deleted in colorectal cancer in dopaminergic neuronal precursor migration, axon guidance, and axon arborization. Neuroscience. 2010; 169:932–949. [PubMed: 20493932]

Yamagata M, Sanes JR. Dscam and Sidekick proteins direct lamina-specific synaptic connections in vertebrate retina. Nature. 2008; 451:465–469. [PubMed: 18216854]

Yamahachi H, Marik SA, McManus JN, Denk W, Gilbert CD. Rapid axonal sprouting and pruning accompany functional reorganization in primary visual cortex. Neuron. 2009; 64:719–729. [PubMed: 20005827]

Yu J-Y, DeRuiter SL, Turner DL. RNA interference by expression of short-interfering RNAs and hairpin RNAs in mammalian cells. Proceedings of the National Academy of Sciences of the United States of America. 2002; 99:6047–6052. [PubMed: 11972060]

Yu W, Baas PW. Changes in microtubule number and length during axon differentiation. J Neurosci. 1994; 14:2818–2829. [PubMed: 8182441]

Zhu H, Hummel T, Clemens JC, Berdnik D, Zipursky SL, Luo L. Dendritic patterning by Dscam and synaptic partner matching in the Drosophila antennal lobe. Nat Neurosci. 2006; 9:349–355. [PubMed: 16474389]

Highlights

Note: DSCAM, Down syndrome cell adhesion molecule; DCC, deleted in colorectal cancer; MTs, microtubules

- DSCAM directly interacts with TUBB3 in a Netrin-1 dependent manner.
- DSCAM collaborates with DCC in Netrin-1-induced binding to TUBB3.
- Netrin-1 increases the colocalization of TUBB3 with DSCAM and DCC in axon branches.
- Netrin-1 induces the interaction of DSCAM with polymerized TUBB3 in MTs.
- DSCAM, DCC and TUBB3 are required for Netrin-1-induced axon branching.

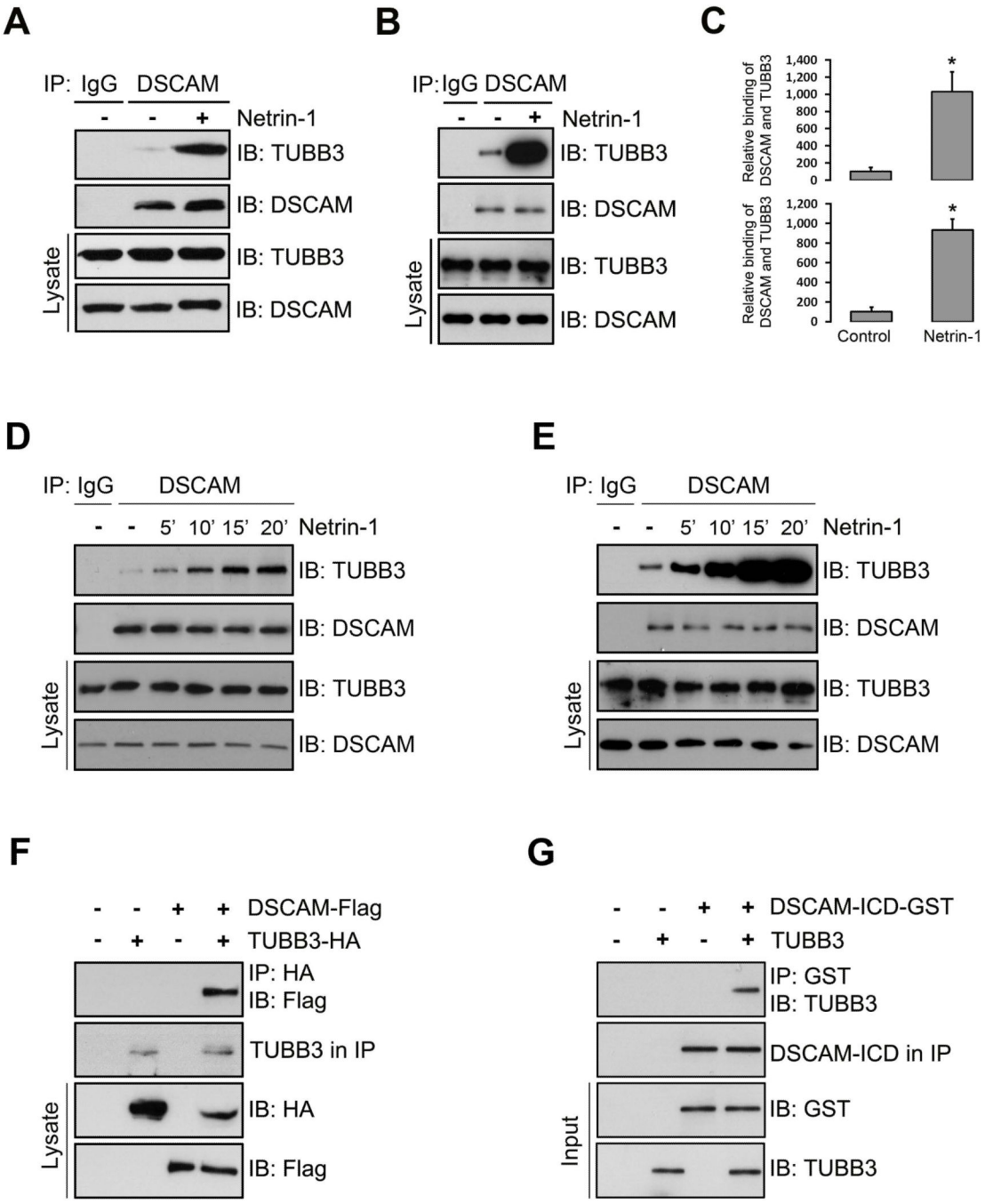

Figure 1.

Interaction of DSCAM with TUBB3. (A–B) Interaction of endogenous DSCAM with TUBB3 in primary neurons. Dissociated E15 mouse cortical neurons (A) and E13 dorsal spinal cord neurons (B) were stimulated with Netrin-1 for 20 min. The anti-DSCAM antibody was used to immunoprecipitate DSCAM proteins and the blot was analyzed with the anti-TUBB3 antibody. (C) Quantification of A (upper panel) and B (lower panel) from three independent experiments. The y-axis shows relative binding of DSCAM with TUBB3 in arbitrary units. * indicates $p < 0.05$ (Student's *t* test). (D–E) Netrin-1 increased the

interaction of endogenous DSCAM with TUBB3 in a time-dependent manner. Primary E15 cortical (D) and E13 dorsal spinal cord neurons (E) were treated with Netrin-1 from 5 to 20 minutes. Lysates of dissociated neurons were immunoprecipitated with anti-DSCAM and analyzed with anti-TUBB3. (F) DSCAM interacts with TUBB3 in HEK293 cells. HEK293 cells were transfected with human full-length TUBB3 tagged with HA only, human full-length DSCAM-Flag only or DSCAM-Flag and TUBB3-HA together. The anti-HA antibody was used to immunoprecipitate TUBB3 and the blot was analyzed with anti-Flag or anti-HA. (G) DSCAM directly interacts with TUBB3. Purified intracellular domain of human DSCAM tagged with GST (DSCAM-GST) was incubated with purified human full length TUBB3 *in vitro*. The anti-GST antibody was used to immunoprecipitate DSCAM-GST and the blot was analyzed with the anti-TUBB3.

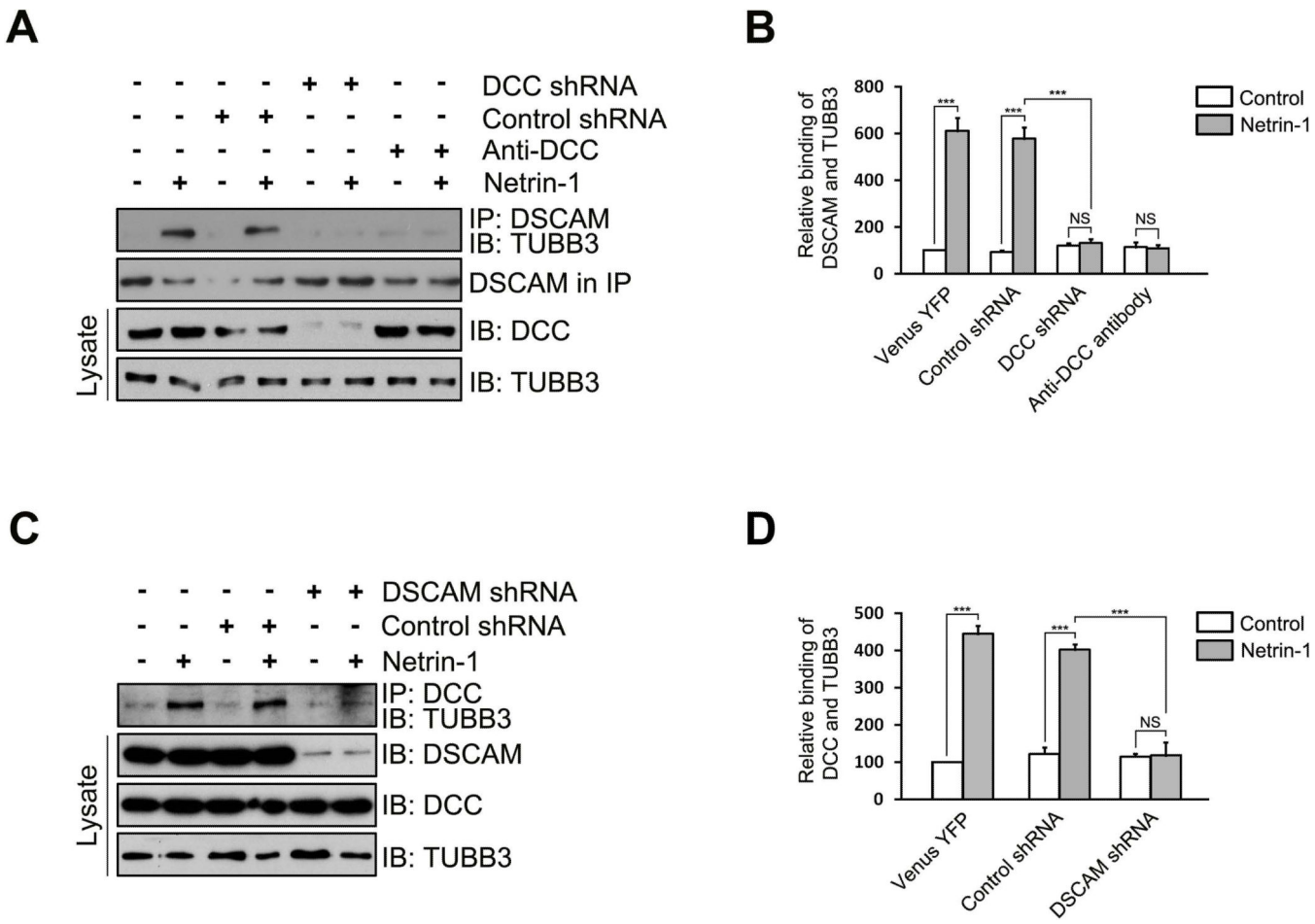

Figure 2.

The coordination of DSCAM and DCC in binding to TUBB3. (A) DCC shRNA or functional blocking anti-DCC antibody inhibited the induction of the interaction of endogenous DSCAM with TUBB3 by Netrin-1. E15 mouse cortical neurons were transfected with Venus YFP only, Venus-YFP plus control shRNA or Venus-YFP plus DCC shRNA and cultured for 2 d. Neurons were stimulated with Netrin-1 or the control in the presence of or absence of anti-DCC functional blocking antibody. (B) Quantification of relative binding of DSCAM and TUBB3. The y-axis shows relative binding of TUBB3 with DSCAM in arbitrary units. Data are mean ± s.e.m from three independent experiments. *** indicates $p < 0.001$ (One way Anova and Fisher LSD post-hoc comparisons). NS, not significant. (C) DSCAM knockdown blocked the Netrin-1-induced interaction of endogenous DCC and TUBB3. E15 mouse cortical neurons were transfected with Venus YFP only, Venus-YFP plus control shRNA or Venus-YFP plus DSCAM shRNA and stimulated with Netrin-1 or the control. Expression of DSCAM shRNA had no effects on levels of endogenous DCC and TUBB3. (D) Quantification of relative binding of DCC and TUBB3. The y-axis shows relative binding of TUBB3 with DCC in arbitrary units. Data are mean ± s.e.m from three independent experiments. *** indicates $p < 0.001$ (One way Anova and Fisher LSD post-hoc comparisons). NS, not significant.

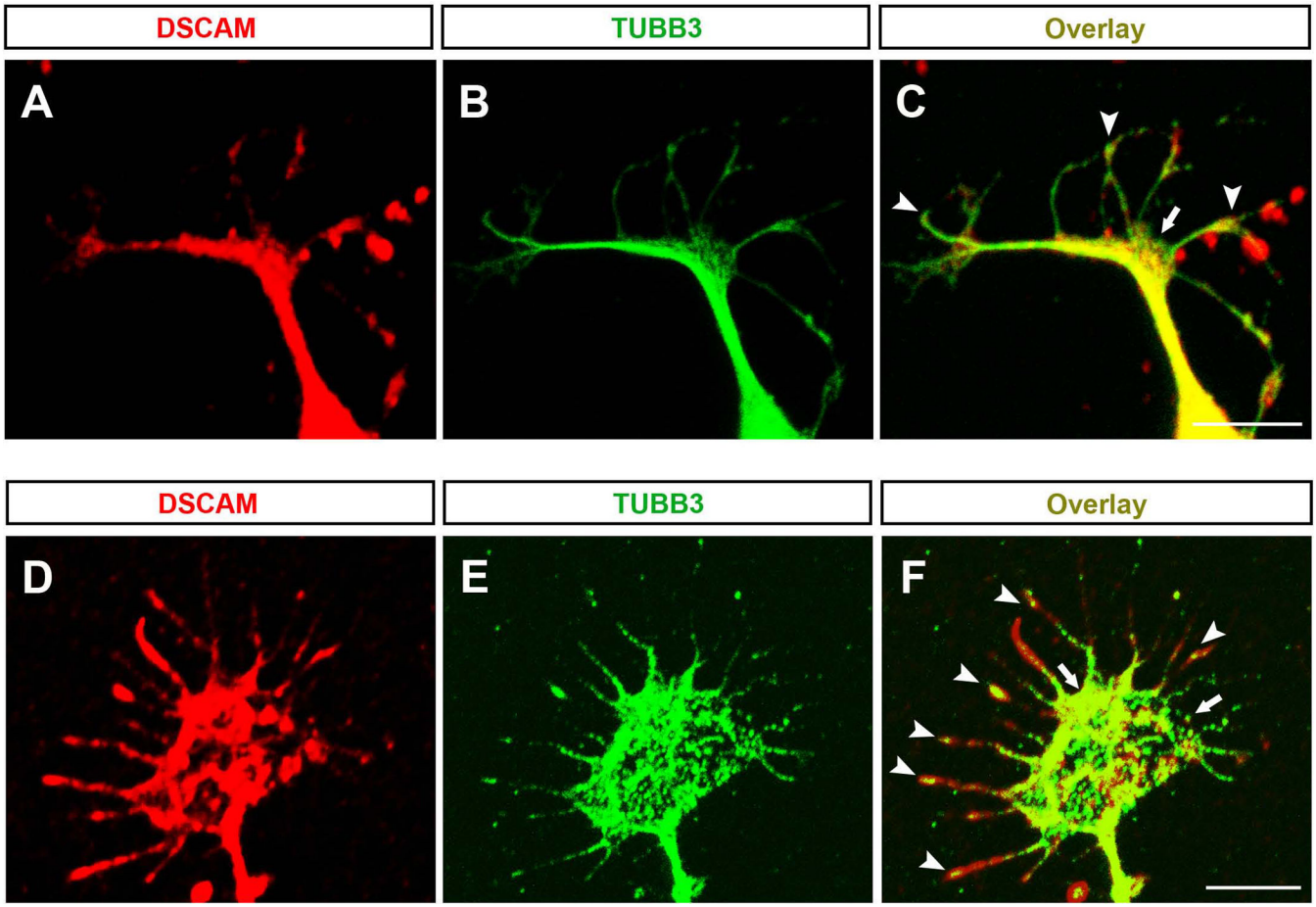

Figure 3.

Subcellular colocalization of DSCAM with TUBB3 in the growth cone of primary neurons. (AC) DSCAM overlapped with TUBB3 in the growth cone of E15 mouse cortical neurons. Panel C is the merged image of A and B, showing overlap both in filopodia (white arrowheads) and lamellipodia (white arrows). The value of PCC of DSCAM and TUBB3 in the peripheral region of axon growth cones in A–C is 0.8 ± 0.1 (mean ± SD). (D–F) DSCAM overlapped with TUBB3 in the growth cone of commissural neuron culture (4 days) from E11 mouse spinal cord. Panel F is the merged image of D and E, showing overlaps both in lamellipodia (white arrows) and filopodia (white arrowheads). The value of PCC of DSCAM and TUBB3 in the peripheral region of growth cones in D-F is 0.7 ± 0.1 (mean ± SD). Scale bar, 10 μm.

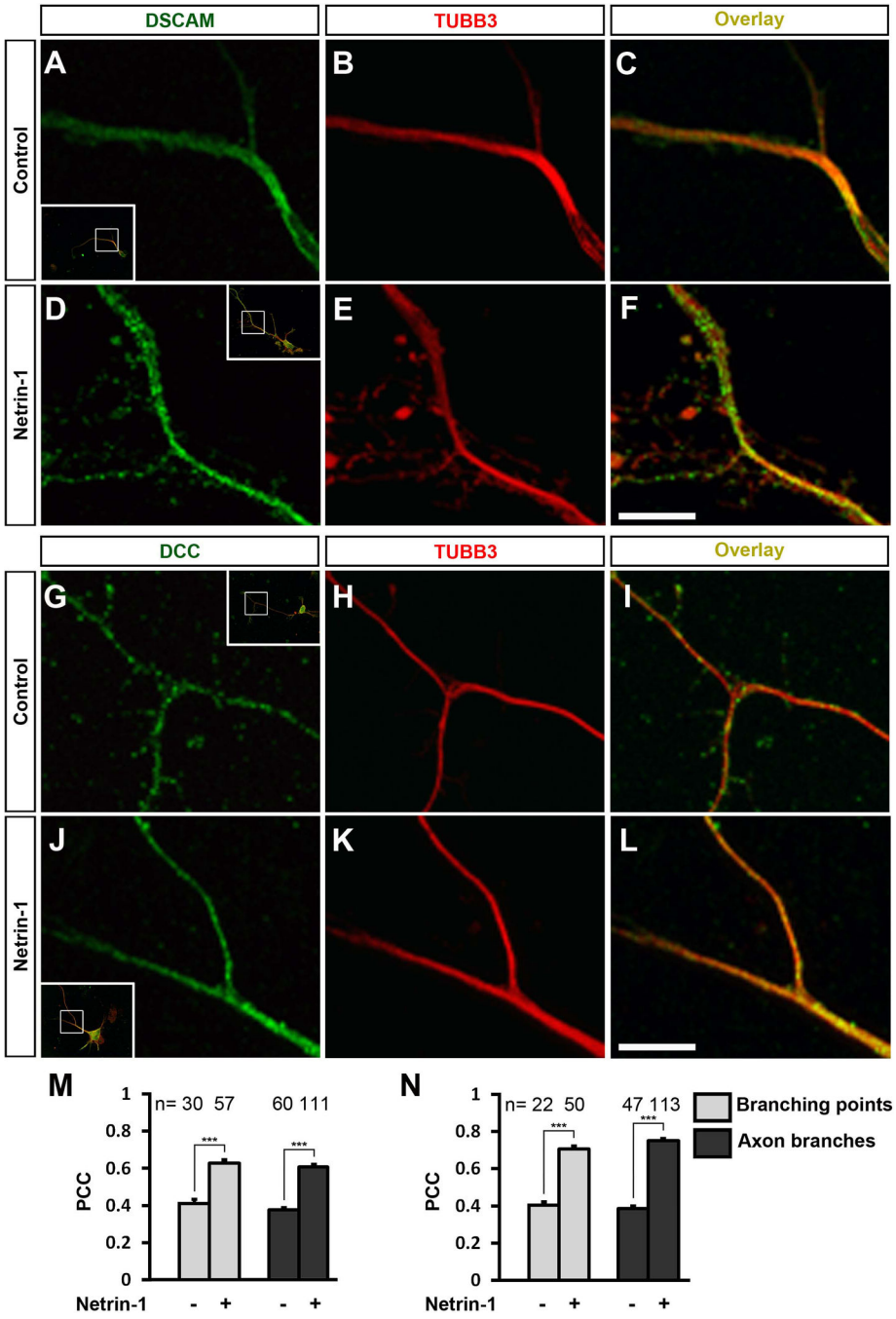

Figure 4.

Subcellular colocalization of DSCAM and DCC with TUBB3 in the axon branches and branching points of primary neurons. (A–F) Overlap of DSCAM (A, D) and TUBB3 (B, E) in axon branches and branching points of dissociated E15 mouse cortical neurons (inserts in A and D) in the presence (D–F) or absence (A–C) of Netrin-1. C is the merged images of A and B. F is the merged image of D and E. Scale bar, 5 μm. (G–L) Overlap of DCC (G, J) and TUBB3 (H, K) in axon branches and branching points of dissociated E15 mouse cortical neurons (inserts in G and J) in the presence (J–L) or absence (G–I) of Netrin-1. I is the

merged images of G and H. L is the merged image of J and K. The boxed insets in A, D, G and J represent the axon branching regions of primary E15 cortical neurons amplified in A–C, D–F, G–I and J–L, respectively. Scale bar, 5 μm. (M–N) Quantitative analysis of Pearson's Correlation Coefficient (PCC). The PCC of TUBB3 with DSCAM (M) and DCC (N) in the axon branches and branching points of E15 mouse cortical neurons was examined by the Leica confocal colocalization analysis software. For quantification, the branching point with a branch longer than 10μm was selected. Netrin-1 dramatically increased the PCC of TUBB3 with DSCAM (M) and DCC (N) in the axon branches and branching points of E15 mouse cortical neurons. *** indicates $p<0.001$ (Student's t test). The numbers on the top (n) indicate the numbers of each group examined.

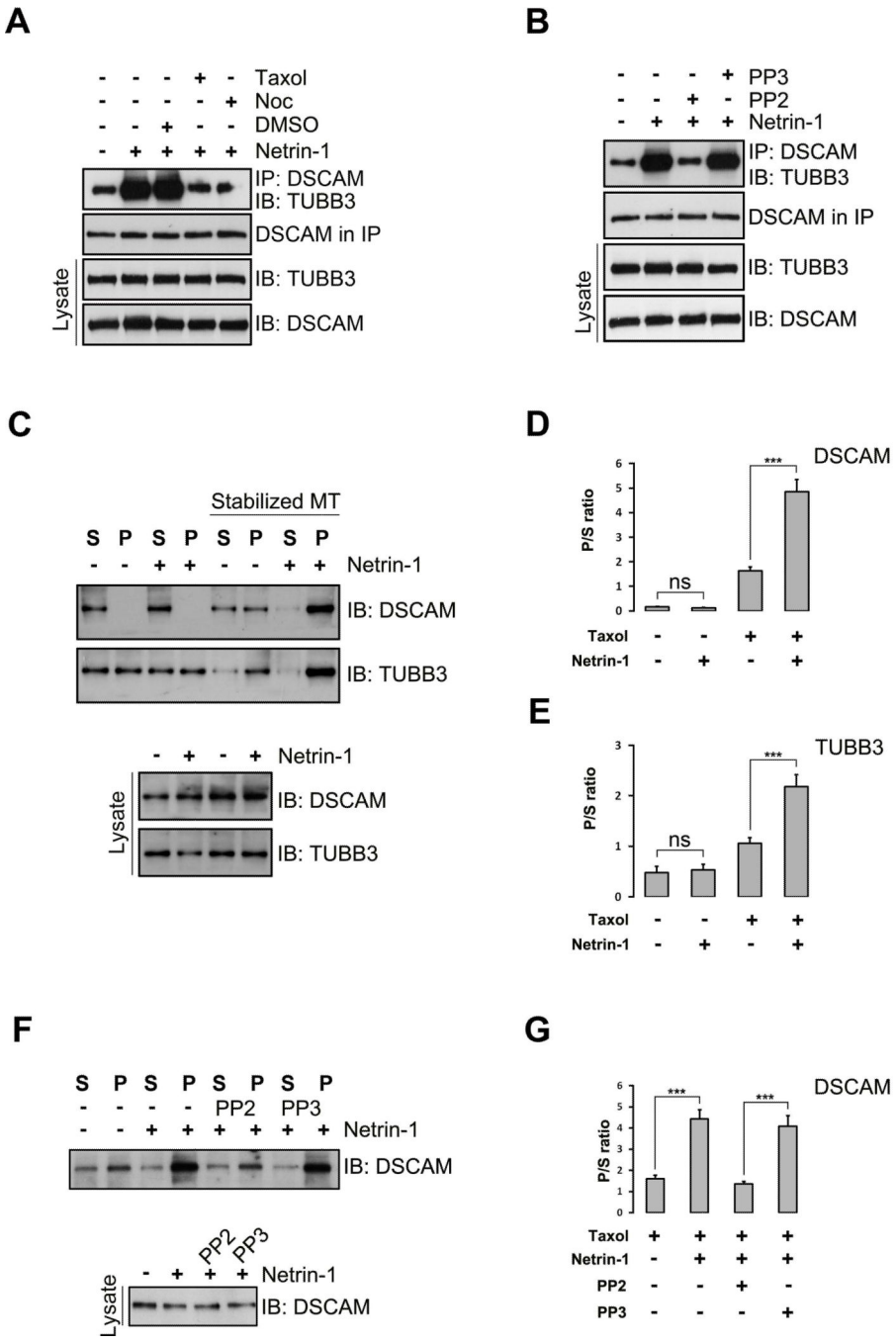

Figure 5.

The induction of the interaction of DSCAM with TUBB3 by Netrin-1 depends on microtubule dynamics and SFK activities. (A) Taxol and nocodazole inhibited Netrin-1-induced interaction of endogenous TUBB3 with DSCAM. E15 cortical neurons were treated with purified Netrin-1 in the presence of 1μM taxol or 3μM nocadozole. The interaction of DSCAM with TUBB3 was determined by immunoprecipitation (IP) with anti-DSCAM and immunoblotting (IB) with the anti-TUBB3. (B) PP2, but not PP3, abolished Netrin-1-induced interaction of endogenous DSCAM with TUBB3 in primary neurons. E15 mouse

cortical neurons were stimulated with purified Netrin-1 in the presence of PP2 or PP3. (C) Netrin-1 increased the cosedimentation of DSCAM and TUBB3 with polymerized MTs in primary neurons. E15 cortical neurons were stimulated with Netrin-1 and MTs in cell lysates were stabilized in the presence of taxol. DSCAM and TUBB3 in the pellet and supernatant fractions were examined by IB with anti-DSCAM and anti-TUBB3, respectively. (D–E) Quantification of C from three independent experiments showing P/S ratio of DSCAM (D) and TUBB3 (E). NS, not significant; ***, $p<0.001$ (One way Anova and Fisher LSD post-hoc comparisons). (F) PP2, but not PP3, blocked Netrin-1-induced cosedimentation of endogenous DSCAM in primary neurons. E15 mouse cortical neurons were stimulated with purified Netrin-1 in the presence of PP2 or PP3. Taxol-stabilized microtubules in cell lysates were separated by centrifugation and DSCAM in the pellet and supernatant fractions was examined by anti-DSCAM. (G) Quantification of F from three independent experiments. ***, $p<0.001$ (One way Anova and Fisher LSD post-hoc comparisons).

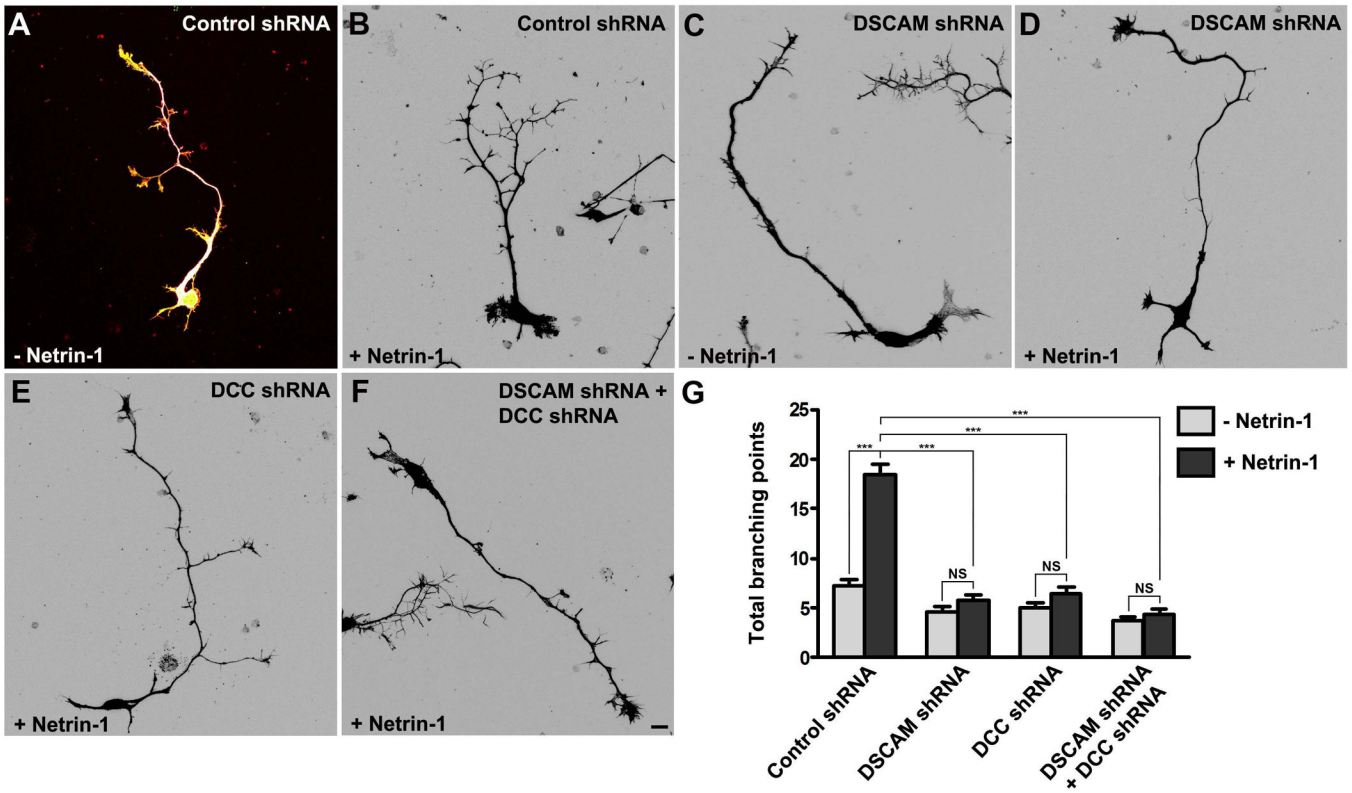

Figure 6.

DSCAM collaborates with DCC in Netrin-1-induced axon branching. (A–F) E15 mouse cortical neurons were transfected with Venus YFP plus control shRNA (A–B), Venus YFP plus DSCAM shRNA (C–D), Venus YFP plus DCC shRNA (E), and Venus YFP plus DC shRNA and DSCAM shRNA (F), respectively. Primary neurons were cultured in the presence (B, D, E–F) or absence (A and C) of purified Netrin-1 for 4 d and stained with anti-tau, phalloidin (F-actin) and DAPI. Images (B–F) are inverted LUT (look-up table) from original RGB pictures. Scale bar, 10 μm. (G) Quantification of Netrin-1-induced axon branching. The branching point with a branch longer than 10μm was selected. Only axon branching points of YFP-positive neurons not in contact with other cells were measured and used in the statistical analyses. More than 80 neurons from three separate experiments were calculated. Data are mean ± s.e.m. ***, $p<0.001$ (One-way ANOVA with Kruskal–Wallis test for post-hoc comparisons). NS, not significant.

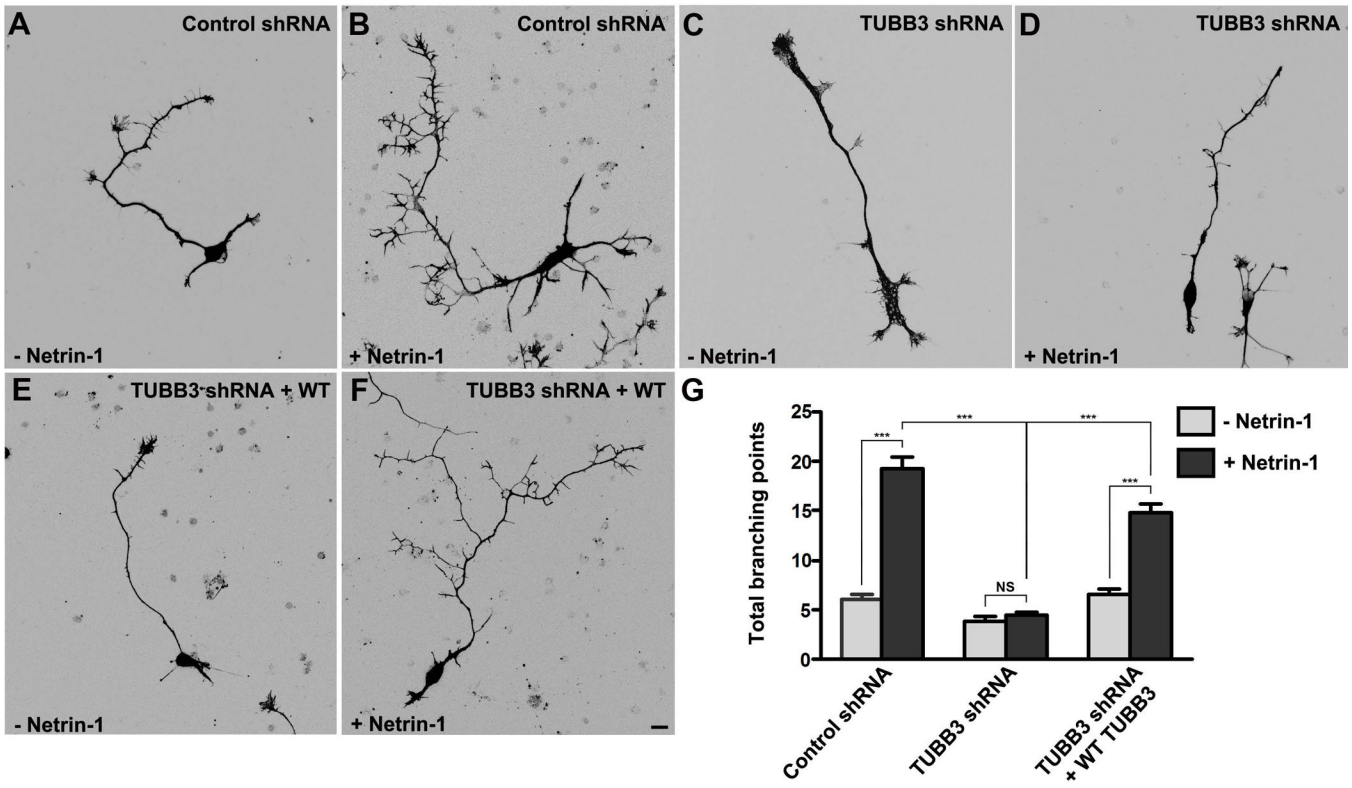

Figure 7.

TUBB3 is involved in Netrin-1-induced axon branching. (A–F) E15 mouse cortical neurons were nucleofected with Venus YFP plus control shRNA (A–B), Venus YFP plus TUBB3 shRNA (C–D), or Venus YFP plus TUBB3 shRNA and wild type human TUBB3 and incubated with (B, D and F) or without (A, C and E) purified Netrin-1 for 4 d. Expression of TUBB3 shRNA inhibited the cortical axon branches induced by Netrin-1 (A–D). The wild type TUBB3 could partially rescue the defect of TUBB3 shRNA knockdown on Netrin-1-induced axon branching (C–F). Scale bar, 10 μm. (G) Quantification of total axon branching points of E15 cortical neurons. Data are mean ± s.e.m. ***, $p<0.001$ (One-way ANOVA with Kruskal–Wallis test for post-hoc comparisons). The numbers of neurons tested were: 92 for the Venus YFP + control shRNA group in the absence of Netrin-1; 88 for the Venus YFP + control shRNA with Netrin-1; 88 and 87 for the Venus YFP + TUBB3 shRNA group in the presence and absence of Netrin-1, respectively; 90 and 80 for the the Venus YFP + TUBB3 shRNA + wild type human TUBB3 group in the absence and presence of Netrin-1.